

ACCESS: Enabling an Improved Flux Scale for Astrophysics

Mary Elizabeth Kaiser, Jeffrey W. Kruk, Stephan R. McCandliss, David J. Sahnou, Robert H. Barkhouser, W. Van Dixon, Paul D. Feldman, H. Warren Moos, Joseph Orndorff, Russell Pelton, Adam G. Riess^{1,3}

¹Department of Physics and Astronomy, Johns Hopkins University, 3400 North Charles Street, Baltimore, MD, USA 21218

Bernard J. Rauscher, Randy A. Kimble, Dominic J. Benford, Jonathan P. Gardner, Robert J. Hill, Bruce E. Woodgate

²NASA Goddard Space Flight Center, Greenbelt, MD USA 20771;

Ralph C. Bohlin, Susana E. Deustua

³Space Telescope Science Institute, San Martin Drive, Baltimore, MD, USA 21218

Robert Kurucz

Harvard Smithsonian Center for Astrophysics, Garden Street, Cambridge, MD, USA 02139;

Michael Lampton

Space Sciences Laboratory, 7 Gauss Way, Berkeley, CA 94720;

Saul Perlmutter

University of California, Berkeley, Berkeley, CA 94720;

Edward L. Wright

University of California, Los Angeles, Los Angeles, CA 90095

ABSTRACT

Improvements in the precision of the astrophysical flux scale are needed to answer fundamental scientific questions ranging from cosmology to stellar physics. The unexpected discovery^{1,2} that the expansion of the universe is accelerating was based upon the measurement of astrophysical standard candles that appeared fainter than expected. To characterize the underlying physical mechanism of the “Dark Energy” responsible for this phenomenon requires an improvement in the visible-NIR flux calibration of astrophysical sources to 1% precision. These improvements will also enable large surveys of white dwarf stars, e.g. GAIA,³ to advance stellar astrophysics by testing and providing constraints for the mass-radius relationship of these stars.

ACCESS (Absolute Color Calibration Experiment for Standard Stars)⁴ is a rocket-borne payload that will enable the transfer of absolute laboratory detector standards from NIST to a network of stellar standards with a calibration accuracy of 1% and a spectral resolving power of $R = 500$ across the 0.35-1.7 μm bandpass.

Among the strategies being employed to minimize calibration uncertainties are: (1) judicious selection of standard stars (previous calibration heritage, minimal spectral features, robust stellar atmosphere models), (2) execution of observations above the Earth’s atmosphere (eliminates atmospheric contamination of the stellar spectrum), (3) a single optical path and detector (to minimize visible to NIR cross-calibration uncertainties), (4) establishment of an a priori error budget, (5) on-board monitoring of instrument performance, and (6) fitting stellar atmosphere models to the data to search for discrepancies and confirm performance.

Keywords: ACCESS, standard stars, calibration, photometry, spectrophotometry, dark energy, Vega, Sirius, BD+17°4708, HD37725, NIST, sub-orbital, rocket, optical spectroscopy, NIR spectroscopy

Send correspondence to M. E. Kaiser: E-mail: kaiser@pha.jhu.edu

1. INTRODUCTION

Current astrophysical problems need a precise (better than 1%) network of astrophysical flux standards spanning a wide dynamic range across the visible and near-infrared (NIR) bandpass to address fundamental questions (e.g. the character of the expansion history of our universe) with the required uncertainty.⁵

However, overall uncertainties in the astrophysical flux scale exceed 1% in the spectral range extending from the ultraviolet through the NIR. And, although isolated spectral regions may achieve 1% levels of precision, it is uncertain if the absolute calibration in those spectral regions is accurate to 1%.

Technological advances in detectors, instrumentation, and the precision of the fundamental laboratory standards used to calibrate these instruments have not been transferred to the fundamental astrophysical flux scale across the visible to NIR bandpass. Furthermore, the absolute normalization of the current astrophysical flux scale is tied to a single star, Vega, a star that is too bright to be observed with today’s premier optical telescopes.

Systematic errors associated with problems such as dark energy now compete with the statistical errors and thus limit our ability to answer fundamental questions in astrophysics.

The scientific impetus for the ACCESS program arose from the discovery of the accelerated expansion of the universe. These results^{6,7,8,9} compared the standardized brightness of high redshift ($0.18 < z < 1.6$) Type Ia supernovae (SNe Ia) to low-redshift SNe Ia,^{10,1,2} showing that at a given redshift the peak brightness of SNe Ia is fainter than predicted. The most plausible explanation for the unexpected faintness of these standard candles is that they are further away than expected, indicating a period of accelerated expansion of the universe and, hence, the presence of a new, unknown, negative-pressure energy component - dark energy. Using SNe Ia to distinguish dark energy models from one another levies a requirement for 1% precision in the cross-color calibration of the SNe Ia flux across a bandpass extending from $0.35 - 1.7 \mu\text{m}$.

Since then, several classes of observationally testable models have been proposed to explain the nature of the dark energy. Accurate testing of models through observation of SNe Ia depends on the precise determination of the relative brightness of the SNe Ia standard candles. For each supernova, its redshift,

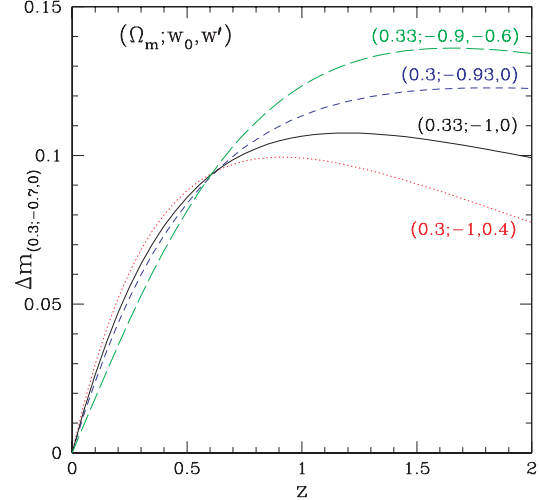


Figure 1. Differential magnitude-redshift diagram for dark energy models with Ω , w_0 , and $w' = xw_a$.¹¹ Note that the models do not begin to distinguish themselves from one another until $z \sim 1$ and the difference between models is of order 0.02 magnitudes (roughly 2%) at $z \sim 2$.

z , is plotted against its rest-frame B-band flux to determine the SNe Ia Hubble brightness-redshift relationship. Cosmological and dark energy parameters are determined from the shape, not the absolute normalization, of this relationship. Since the rest-frame B-band is seen in different bands at different redshifts, the relative zero-points of all bands from $0.35 \mu\text{m}$ to $1.7 \mu\text{m}$ must be cross-calibrated to trace the supernovae from $z=0$ to $z \sim 1.5$. The term “absolute color calibration” is defined as the slope of the absolute flux distribution versus wavelength. This color calibration must be precise enough to clearly reveal the differences between dark energy models (Figure 1) over this range of redshifts.

Using SNe Ia to distinguish dark energy models from one another levies a requirement for 1% precision in the cross-color calibration of the SNe Ia flux across a bandpass extending from $0.35 - 1.7 \mu\text{m}$.

With the reduction of statistical uncertainties in supernova cosmology, the importance of understanding and controlling systematic uncertainties has gained prominence and is now key to investigating the dark energy properties.¹² Observations of higher redshift SNe Ia are needed to discriminate between different dark energy models, thus motivating an absolute color calibration to 1% precision in the NIR ($1 - 1.7 \mu\text{m}$). Controlling the systematic errors to this level of accuracy and precision is required, not

only for the absolute color calibration, but also for other sources of systematic errors which themselves depend on the color calibration (e.g. extinction corrections due to the Milky Way, the SN host galaxy, and the intergalactic medium, in addition to the K-corrections which provide the transformation between fluxes in the observed and rest-frame passbands).

2. ACCESS OVERVIEW

This program, ACCESS - “Absolute Color Calibration Experiment for Standard Stars”, is a series of rocket-borne sub-orbital missions and ground-based experiments that will enable the absolute flux for a limited set of primary standard stars to be established using calibrated detectors as the fundamental metrology reference. These experiments are designed to obtain an absolute spectrophotometric calibration accuracy of $< 1\%$ in the $0.35 - 1.7 \mu\text{m}$ bandpass at a spectral resolution greater than 500 by directly tracing the observed stellar fluxes to National Institute of Standards and Technology (NIST) irradiance standards. Transfer of the NIST detector standards to our target stars will produce an absolute calibration of these standards in physical units, including the historic absolute standard Vega.

ACCESS will reduce uncertainties in the current standard star calibration system through careful attention to details, both large and small, that can impact the success of this project. In designing this program we have sought to identify and ameliorate potential sources of error that could prohibit achieving a 1% calibration. As a result, we have (1) targeted the judicious selection of standard stars. Only existing (known) standard stars with previous calibration heritage will be observed. Selection criteria include restrictions to spectral classes that exhibit minimal spectral features and for which robust stellar atmospheres models are available (e.g. pure DA white dwarf stars, AV stars). (2) Stellar atmosphere modeling of our measurements will provide an important cross-check on the observations and enable the extension of these measurements to wavelengths outside our observed bandpass. Within the signal-to-noise constraints of the observations, standard stars with flux levels extending to $\sim 10^{\text{th}}$ magnitude will be selected to enable observation by large aperture telescopes and thus eliminate additional calibration transfers.

Uncertainties in the absolute flux will be further minimized by (3) observing above the Earth’s atmo-

sphere and avoiding both atmospheric emission and absorption that presents a severe contaminant to the stellar spectrum longward of $0.85 \mu\text{m}$ at both ground and balloon altitudes. Measurement robustness also benefits from (4) obtaining observations with an instrument that uses a single optical path and detector across its full bandpass of $0.35 - 1.7 \mu\text{m}$, thus eliminating cross-calibration systematic errors. Establishing and tracking (5) an *a priori* error budget, maintains focus on the magnitude of errors that can be tolerated at the sub-system level. Performing NIST traceable sub-system and end-to-end payload calibrations, yields an absolute calibration in addition to the relative calibration that is the focus of many scientific applications. Furthermore, (6) monitoring and tracking payload performance with an on-board monitoring source that utilizes all elements of the optical path enables knowledge of system performance prior to and during payload flight.

Current technology has enabled increased calibration precision for detector-based irradiance standards, providing a factor of two reduction in uncertainties from the previous, source-based, spectral irradiance scale in the visible and even greater improvements are realized in the NIR,^{13,14,15} making standard detectors the fundamental reference calibrator of choice.

And while the full end-to-end calibration of an instrument in physical units with an absolute laboratory standard is preferred, it is not always feasible. Consequently the essence of the ACCESS program is to establish this calibration for the fully integrated telescope and spectrograph and transfer this calibration to the stars using both NIST irradiance standards and the end-to-end NIST SIRCUS^{16,17} calibration facility. As a result, the absolute foundation of the existing network of standards stars, including the standards Vega and Sirius, will be strengthened through accurate, higher resolution, higher precision, broader bandpass measurements extending to lower flux levels. This improved network of standard stars, extending to 10^{th} magnitude, will be available to all telescopes as standard sources.

3. FLUX STANDARDS & CALIBRATION

Ultimately, observed astrophysical fluxes must be converted to physical units. Three of the most common methods of determining the absolute color calibration of stellar fluxes are solar analog stars, stellar atmosphere models, and comparison to certified laboratory standards. The existing precision in

each of these methods is inadequate for dark energy SNe cosmology.

3.1 Solar analog stars

Use of solar analog stars as a standard source relies upon the star having the same intrinsic spectral energy density (SED) as the sun. Unfortunately, no star is a true solar analog. Even G-type stars with the most-closely matching visible spectra can differ by a few percent. In the NIR, differences in magnetic activity can restrict the accuracy to 5%.¹⁸ In addition, uncertainties in the solar SED itself are 2-3%.¹⁹

3.2 Stellar atmosphere models

Stellar atmosphere models are currently the preferred method for calibrating stellar fluxes due to the agreement between the models and the observations and the increased resolution of both the models and the data. In the ultraviolet and visible region of the spectrum, this calibration network is based on the relatively featureless spectra of unreddened hot white dwarf (WD) stars with pure hydrogen atmospheres. Absolute photometry of Vega is used to normalize the spectral energy distributions of these stars and their stellar models to an absolute flux scale.

Currently, the three primary WD standards of the *HST* CALSPEC network are internally consistent to an uncertainty level of 0.5% in the visible with localized deviations from models rising to $\sim 1\%$ over the 4200 – 4700 Å spectral range,¹⁸ and a $\pm 1\%$ uncertainty in the NIR ($1 - 2 \mu\text{m}$).¹⁸ Thus, the level of agreement between the model and the data is a function of wavelength. Any systematic modeling errors that affect the shape of the flux distributions of all three WD stars equally cannot be ruled out and would make the actual error larger.

Current uncertainties in the extensive NIR ($1.0 < \lambda < 1.7 \mu\text{m}$) network of standard stars are $\sim 2\%$.^{21,22,23}

A recent compilation²⁴ of IR standard star calibrations based on direct absolute measurements and indirect calibrations through modelling and extrapolation/interpolation of observations tests the internal consistency of these measurements and examines the impact of extrapolating the IR data into the visible. The data are found to be consistent, but adjustments of $\sim \pm 2\%$ to published calibrations are recommended and the deviations of Vega from a typical A0V star between the visible and IR are noted and quantified.

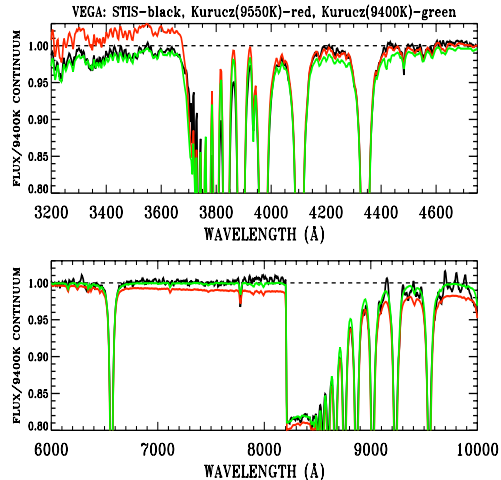


Figure 2. Uncertainties in the absolute flux for Vega: HST/STIS observations^{18, 20} (black line), the Kurucz stellar model with $T_{eff} = 9400$ K (green), and the Kurucz stellar model at 9550 K (red) are compared. The observations exhibit better agreement with the cooler model at the longer and shorter wavelengths. The hotter model agrees better with the measured flux by $\sim 1\%$ at 4200–4700 Å. Vega, a pole-on rotating star, presents a range of temperatures, which introduce added complexity to obtaining a robust stellar model.

3.3 Certified Laboratory Standard Sources

To reduce uncertainties to $< 1\%$, the NIST fundamental laboratory standards must be directly tied to astrophysical sources, i.e. stars, at this level of precision.

Photometric measurements of Vega have been absolutely calibrated against terrestrial observations of certified laboratory standards (e.g. tungsten strip lamps, freezing-point black bodies).²⁵ These absolute photometry experiments provide the normalization for the network of stellar models and templates that are used as practical absolute standards. These absolute calibrations to standard sources were difficult. Observation of the laboratory source using the full telescope was typically achieved by placing the source at a nearby distance ($\sim 200\text{m}$) and correcting for the intervening, non-negligible, air mass. This resulted in errors due to the large and variable opacity of the atmosphere. This methodology is being re-visited using current technology.^{26,27,28} Other programs (e.g. Pan-STARRS, LSST) plan to use dedicated telescopes to simultaneously monitor the atmosphere to provide corrections for the science observations at the neighboring telescope.^{29,30,31}

In the IR, introducing the absolute calibrator at the focal plane of the telescope minimized atmo-

spheric absorption of the laboratory standard,³² but required corrections due to differences in the optical train and atmospheric corrections to the stellar observations.

Discrepancies of $>10\%$ in Vega’s flux exist at $0.9 - 1 \mu\text{m}$, whereas the measurements from $0.5 - 0.8 \mu\text{m}$ agree to $\sim 1\%$.^{20, 25} Beyond $1 \mu\text{m}$, windows of low water vapor absorption have been used for absolute photometry.^{33,34}

The uncertainty in the standard star flux calibration network relative to the fundamental laboratory standards currently exceeds 1% .

Certified Detectors:

A calibration methodology based on precisely calibrated photodiode detector standards is advocated³⁵ given the limitations and challenges imposed by atmospheric transmission and radiance standards in achieving 1% photometry from the ground. The calibration precision and stability of photodetectors has greatly improved since early pioneering measurements.^{36,37} NIST $\sim 2\sigma$ uncertainties in the absolute responsivity of standard detectors are $\sim 0.2\%$ for Si photodiodes and 0.5% for NIR photodiodes.³⁸ This increased precision in the photodetector calibration, ease of use, and repeatability, now make standard detectors the calibrator of choice.

3.4 Observing Strategy

A rocket platform was selected for the ACCESS observations because the rocket flies completely above the Earth’s atmosphere, thus eliminating the challenging problem of measuring the residual atmospheric absorption and strong atmospheric emission seen by ground-based observations and even by observations conducted at balloon altitudes. A high-altitude balloon flying at 39 km is above 99% of the atmospheric water vapor (the primary source of absorption at these wavelengths), but this is still well below most of the source of the time-variable OH airglow emission, which originates in a $6 - 10 \text{ km}$ layer at an altitude of $\sim 89 \text{ km}$.³⁹ This forest of emission lines, extending from $0.85 \mu\text{m}$ to $2.25 \mu\text{m}$, is much stronger than the continuum flux from a 13^{th} mag star. The number, strength, and variability of these lines has implications for increased statistical noise and systematic effects resulting from subtraction of the OH background in addition to the challenge of eliminating the strong scattered light within the instrument arising from these lines.

In order to improve on the limited precision of models and directly tie our fluxes for the bright stars Vega and Sirius to the fainter stars needed for large telescopes, the $V=8.4 \text{ mag}$ Spitzer/IRAC standard HD 37725⁴⁰ and the $V=9.5 \text{ mag}$ Sloan Digital Sky Survey (SDSS) standard BD+17°4708 will be observed as primary targets. Using a rocket platform, observing time above atmosphere is limited to ~ 400 seconds. Consequently, standard star selection was constrained to targets brighter than 10^{th} magnitude.

BD+17°4708 has precisely established fluxes on the *HST* WD scale⁴¹ and will tie both the HST and SDSS networks directly to the NIST flux scale. The fluxes for Vega and BD+17°4708 were measured by STIS; and the sensitivity of our payload is sufficient to confirm the flux ratio of BD+17°4708/Vega with a S/N of 1% . NIR spectrophotometry of the historically fundamental standard, Vega, whose flux at 5556 \AA sets the absolute level for all standard star networks, has not yet been done. Observations of Vega and Sirius are also essential for tying the NIST fluxes to the extensive Cohen IR network.^{21,22,23}

Models for all the targets observed by ACCESS will be computed to confirm the consistency of our observations over $0.35 - 1.7 \mu\text{m}$ and to provide an extension to other wavelengths.

Two flights are required for each of the two observing fields (Vega + BD+17°4708; Sirius + HD 37725) to verify repeatability to $< 1\%$, which is essential for proving the establishment of standards with 1% precision.

4. ACCESS TELESCOPE AND SPECTROGRAPH

The ACCESS telescope is a Dall-Kirkham cassegrain design with aluminum and fused silica over-coated Zerodur mirrors. The telescope feeds a low-order echelle spectrograph with a cooled, substrate-removed, HgCdTe detector.

The telescope optical bench has flown a number of times. It consists of an invar primary mirror base-plate with a cantilevered invar tube, which serves as both a heat shield and mounting structure for the secondary mirror and a co-aligned star tracker. The optical bench sits on thermal insulating pads and is bolted to a radex joint to which the outer rocket skins are attached. The “thermos bottle” configuration of rocket skin and inner heat shield provides the thermal isolation required to keep the primary and secondary vertex-to-vertex distance fixed to less than 0.001 inch for the duration of the flight.

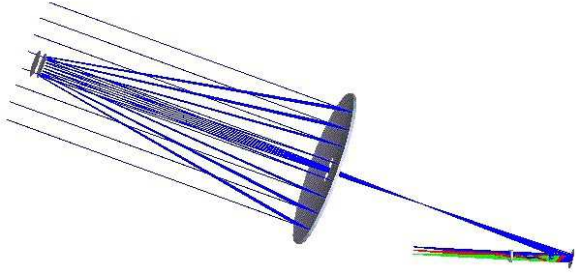


Figure 3. Raytrace view of ACCESS. Parallel rays from the star enter the Dall-Kirkham Cassegrain telescope at left and are incident on the primary mirror (center of figure). The telescope secondary is at left in the figure and the grating is the optical surface at the extreme right in the figure.

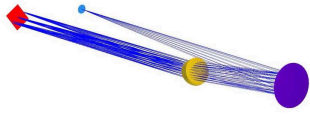


Figure 4. Raytrace view of the ACCESS spectrograph illustrating the grating on the right, the cross-dispersing prism, and the first three orders dispersed by the grating and incident on the detector at left.

The spectrograph is configured as an echelle (Fig. 4) and used in 1st (9000 – 19000 Å), 2nd (4500 – 9500 Å) and 3rd orders (3000 – 6333 Å). It consists of just two optical elements, a concave diffraction grating with a low ruling density, and a prism with spherically figured surfaces placed in the converging beam. The separation of the three orders on the detector is ~1 mm. The resolution of the spectrograph depends on the telescope point spread function (PSF) and the size of the detector pixels. For the telescope PSF of 1.17" (as achieved on recent flights with a similar design) the 18 μm pixels of the detector are critically sampled and produce constant wavelength resolution elements in each order, giving a resolving power ranging between 500 and 1000 (Fig. 5).

The spectrograph housing⁴² will be evacuated and mounted to the back of the primary mirror baseplate. An angled mirrored plate with a 1 mm aperture in the center located at the telescope focus serves as the slit jaw, allowing light to enter the spectrograph while reflecting the region surrounding the target into an image-intensified video camera for real-

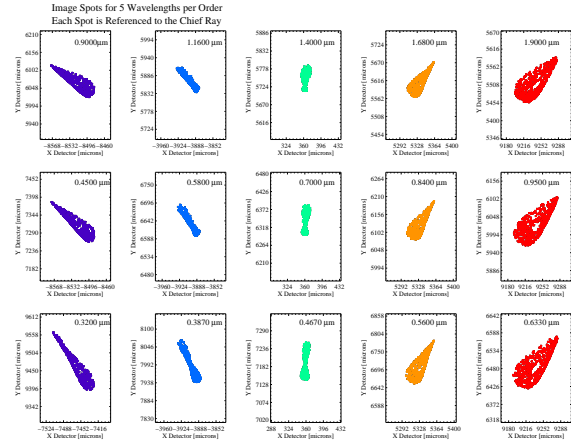


Figure 5. Spot diagrams for an optical layout at a selection of wavelengths spanning the ACCESS bandpass. Each box is labelled in microns and each spot is referenced to the chief ray. In general, the ray trace yields 1×4 pixel images at the blaze wavelength, with 18×18 μm pixels.

time viewing and control by the operator on the ground.

The optical elements are sealed in a stainless steel vacuum housing to provide for contamination control, thermal stability, and calibration. A fused silica entrance window sits behind the slit jaw. The detector is mounted on a focus adjustment mechanism, and the grating and cross disperser are mounted inside along with a set of baffles. The spectrograph vacuum is maintained by a non-evaporable getter and is monitored by an ion gauge. The typical vacuum is < 10⁻⁶ Torr.

The focal plane array will be a 1K×1K HgCdTe device, with the composition tailored to produce a long-wavelength cutoff at ~1.7 μm, and the CdZnTe growth substrate removed to provide high NIR quantum efficiency (QE) and response through the visible to the near-ultraviolet (Fig. 6). Pioneered by Teledyne Imaging Sensors (TIS) to enable the HST/Wide Field Camera 3 (WFC3) to operate without a cryocooler, these detectors require a much simpler cooling system than that required by standard HgCdTe detectors with cutoffs at longer wavelengths. The band gap corresponding to the 1.7 μm cutoff yields low dark current at operating temperatures near 145 – 150K and makes the detectors relatively insensitive to thermal background radiation, though moderate cooling of the detector surroundings (the evacuated spectrograph) will be required. While the detector does have a view factor to the warmer telescope optics upstream, these are seen only through the small

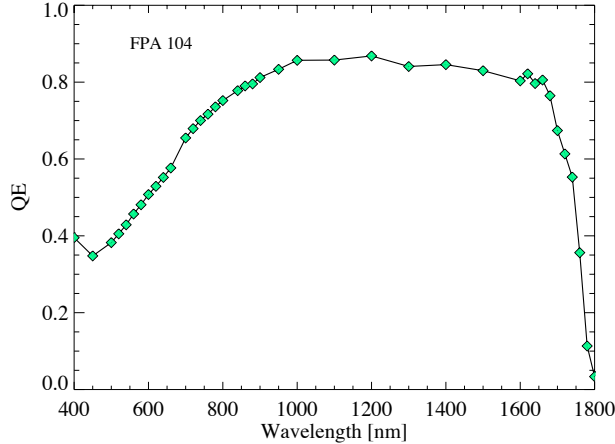


Figure 6. Quantum Efficiency of a flight candidate detector. The increase in signal below 400nm is probably the result of a red leak. These initial measurements were made when the detector was slated for a NIR-only instrument.

slit jaw aperture, reducing their background contribution to acceptable levels.

The detector array is indium bump-bonded to a Hawaii 1-R multiplexer. The resulting device has a format of 1024×1024 pixels, each $18 \mu\text{m} \times 18 \mu\text{m}$ with 1014×1014 active imaging pixels and 5 rows and columns of reference pixels at each edge. The reference pixels are connected to capacitive loads rather than active imaging pixels; they track the effects of thermal drift and low frequency noise that plagued earlier generations of such devices.

Using realistic values to characterize the throughput of the optical components, the grating, and the detector indicates that subsecond integration times will be required to avoid saturation of the detector for the bright stars Sirius and Vega (Fig. 7). Proven algorithms for subarray readouts of the detector will be used to accomplish this.

For the fainter targets, a 400 second observation yields a S/N of 200 per spectral resolution element down to the Balmer edge. Additional binning can further increase the background subtracted signal-to-noise ratio of the acquired spectrum.

5. ACCESS CALIBRATION

5.1 Calibration Overview

The ACCESS calibration program consists of five principal components.

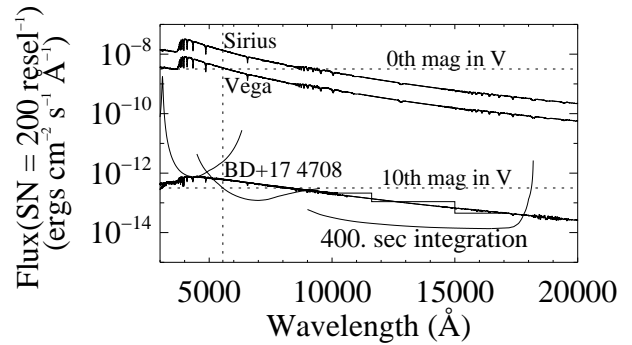


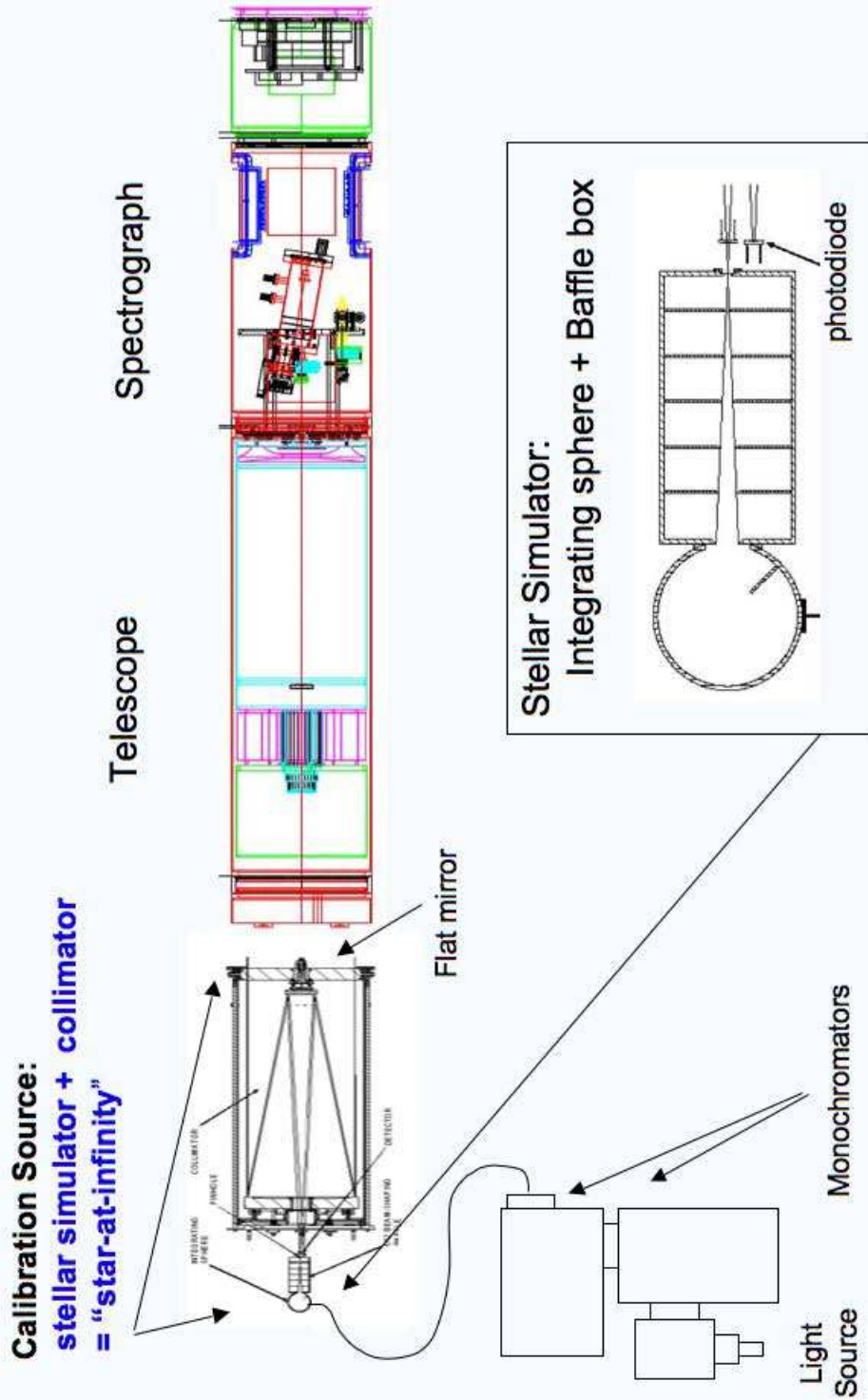
Figure 7. The flux limit for a signal-to-noise of 200 in a 400 second rocket flight is shown for each of the three ACCESS orders. The flux for three selected targets is overplotted for comparison. Except at the very shortest wavelengths for BD+17° 4708, a signal-to-noise ratio of 200 is achievable at a resolving power of 500 in a single rocket flight.

1. Establish a standard candle that can be traced to a NIST detector-based irradiance standard.
2. Transfer the NIST calibrated standard(s) to the ACCESS payload - calibrate the ACCESS payload with NIST certified detector-based laboratory irradiance standards.
3. Transfer the NIST calibrated standard(s) to the stars - observe the standard stars with the calibrated ACCESS payload.
4. Monitor the ACCESS sensitivity - track system performance in the field prior to launch, while parachuting to the ground, and in the laboratory, to monitor for changes in instrument sensitivity.
5. Fit stellar atmosphere models to the flux calibrated observations - confirm performance, validate and extend standard star models.

Determination of the ACCESS instrument sensitivity is, in principle, a simple process of knowing the ratio of the total number of photons entering the telescope aperture to the total number of photons detected by the spectrograph detector as a function of wavelength.

Quantification of the number of photons entering the telescope requires a source with a known number of photons in a beam matched to the entrance aperture of the telescope. For ACCESS, this source (Fig. 8) will consist of a stellar simulator and a

ACCESS Ground Calibration



collimator to provide the “star-at-infinity” required by the telescope. The stellar simulator (Fig. 8) will be comprised of a pinhole placed at the collimator focus and fed by an integrating sphere baffled to match the focal ratio of the collimator. To ensure spectral purity, the integrating sphere is fed by a fiber optic coupled to the output of a dual monochromator.

Knowledge of the total number of photons in the output beam of the collimator, which is the input beam to the telescope, will be provided by two measurements. The first is a simple measurement of the intensity of the light passing through the pinhole of the stellar simulator by a NIST calibrated photodiode transfer standard and the second is a measurement of the reflectivity of the collimator (§ 5.2).

The end-to-end calibration of the telescope with spectrograph may then be performed as a function of wavelength by simply measuring the intensity of the simulated star, measuring the count rate at the spectrograph detector, and correcting for the collimator attenuation of the simulated star.

The signal measured from the stellar simulator by the photodiode is a radiant flux (power) and has units of erg s^{-1} . The signal from the star is an irradiance, and has units of $\text{erg s}^{-1}\text{cm}^{-2}$. The calibrated irradiance is then obtained after precise measurement of the telescope primary and secondary mirror dimensions and dividing the calibrated radiant flux by the illuminated area of the primary mirror.

Although simple in principle, systematic effects, such as the uniformity of reflective coatings, matching of the collimator and telescope apertures, the spatial uniformity of the photodiode detectors, the transmission of the slit, the scattered light determination, the determination of the area of the primary and secondary telescope mirrors, the stability of the light source, etc., must be closely tracked if this process is to yield the required precision and accuracy.

5.2 NIST Absolute Calibration Transfer

Standard Detectors Two types of NIST-calibrated standard photodiodes will be required to calibrate the spectral range of the ACCESS instrument from $3500 \text{ \AA} - 1.7 \mu\text{m}$. A thirteen year pedigree of stability dictates our choice of a Si photodiode in the visible. In the NIR, an InGaAs photodiode will be used. NIST will measure the absolute spectral responsivity and map the spatial uniformity for each photodiode.

The relative expanded uncertainty ($\sim 2\sigma$) error of the absolute responsivity of the Si photodiodes is $\sim 0.2\%$.³⁸ With the NIST Spectral Comparator Facility (SCF), the spectral responsivity of the NIR photodetectors can be measured with a combined relative standard uncertainty of less than 0.4% .^{43,38}

Collimator A vacuum grade collimator, under nitrogen purge, will be used to illuminate and characterize the ACCESS instrument in a darkroom environment. Determination of the collimator throughput will be achieved by using the collimator in double-pass with the stellar simulator. The double pass configuration (DPC) consists of the primary and secondary collimator mirrors in combination with a high quality flat mirror (Fig 8). Measurement of the reflectivity of the flat mirror and the input and output signal of the stellar simulator will result in the determination of the reflectivity product of the primary and secondary mirrors.

Measurement of the Reflectivity of the Flat

The relative reflectivity of the flat mirror will be measured as a function of wavelength using a monochromator. This relative measurement is transferred to an absolute reflectivity measurement through the measurement of the witness samples in concert with the flat at each wavelength. These measurements are performed inside a clean tent under nitrogen gas purge in a dark room to maintain cleanliness and a low light level environment. The photodiodes are cooled for stability and low dark current. The source is operated in a thermally controlled housing with a radiometric power supply which controls the light ripple to $\leq 0.4\%$. A monitoring diode will track any variations in the source output during the reflectivity measurements and the data will be correspondingly corrected. Background signal measurements, with the source shuttered, will be taken before and after each reflectivity measurement.

Collimator Throughput The second step in the collimator calibration establishes the reflectivity product of the combined primary and secondary mirrors. For this measurement a light source, dual monochromator, spectralon-coated integrating sphere, and F/12 baffle box with pinhole (Fig. 8) combine to generate a stellar simulator, or artificial star, which directly illuminates the DPC. To avoid polarization of the beam, no mirrors fold the beam. Instead, the

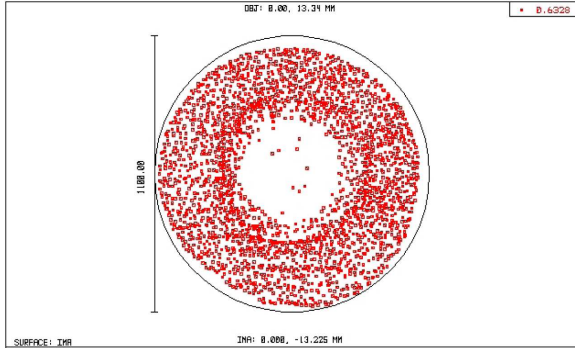


Figure 9. The annular distribution of rays in the image show the collimator beam spot on the photodiode detector. The black circle enclosing these rays depicts the expected size of the NIST beam during the absolute responsivity calibration.

direct measurement of the artificial star and the return measurement of the image after the DPC are accomplished using a rotation stage to place the photodiode into the incident and return beams. We expect an 85% overlap (Fig. 9) in the photodiode area sampled by the stellar simulator and the NIST calibration beam.

A reference photodiode at an output port of the integrating sphere will monitor the source for signal variations. The source will be shuttered and measurements will be taken before and after each measurement to correct for the background signal.

The f-number of the artificial star system will be matched to the f-number of the collimator to ensure that the beam slightly underfills the full aperture of the collimator. From measurements of the artificial star input and return signals without an aperture stop we determine the efficiency of the collimator.

To ensure that the telescope will be underfilled and no light lost, an aperture stop will be inserted into the collimated beam. The input and return signals will be measured and the size of the aperture stop will be known from prior measurements. Thus the input signal to the telescope is determined.

The uniformity of the illumination at the flat will be checked using a rotating mask with a small sub-aperture in front of the flat and monitoring for diode signal fluctuations. The flat is then removed from the system and the collimator is now used in single pass with the artificial star to illuminate the telescope and determine its end-to-end sensitivity.

Ground Calibration Steps

1. Reflectivity of flat as a function of wavelength.
 - Relative of entire surface, cross-calibrate to witness
 - Absolute calibration of witness
2. Relative calibration of stellar simulator (input beam to telescope).
 - Measure F/12 output of pinhole (artificial star)
 - Measure the return beam from F/12 collimator in double pass off flat.
3. Check uniformity of collimator beam.
 - Scan sub-aperture in auto-collimated configuration
4. Characterize collimator to telescope pupil match.
5. Measure slit losses.
 - Slit-in, slit-out method
 - Direct characterization of PSF with flight array detector in focal plane
6. Measure PSF of telescope spectrograph at spectrograph focal plane.
7. Characterize flat-field response of spectrograph detector.
8. Characterize linearity of spectrograph detector.
9. Characterize linearity of absolute calibration standards.
10. Characterize read noise of the detector.
11. Characterize readout properties of the detector.
12. Absolute calibration of telescope and spectrograph.
 - Measure monochromatic pinhole output into collimator.
 - Measure response of flight array detector at spectrograph focal plane.

Figure 10. Outline of the ground calibration steps.

End-to-end ACCESS instrument throughput

To check for losses at the slit, the instrument will be illuminated with and without the slit and the throughput measured at the telescope focal plane with a photodiode for each case. The results will be compared to verify that slit losses are insignificant as expected with the 1 mm (~ 32 arcsecond) ACCESS slit aperture. This will be checked against a direct measurement of the telescope PSF using the array detector.

Next the PSF will be measured with the array detector at the spectrograph focal plane, again images will be checked for systematic effects. Measurements will be made to check for, characterize, and eliminate sources of scattered light.

The absolute calibration of the telescope can then be determined by measuring the artificial star signal at the pinhole with a NIST calibrated photodiode, then measuring the signal at the ACCESS instrument focal plane with the instrument (spectrograph) detector.

Cross-Checks The primary calibration, described above, uses a NIST precision calibrated photodiode detector standard to map the instrument's sensitivity in a series of monochromatic wavelength steps. A brief outline of calibration that will be performed is presented in Figure 10. After this calibration, the instrument will be transported to NIST where the throughput will be determined using two additional methods. The first method will calibrate the end-to-end sensitivity using the Spectral Irradiance and Radiance Responsivity Calibrations with Uniform

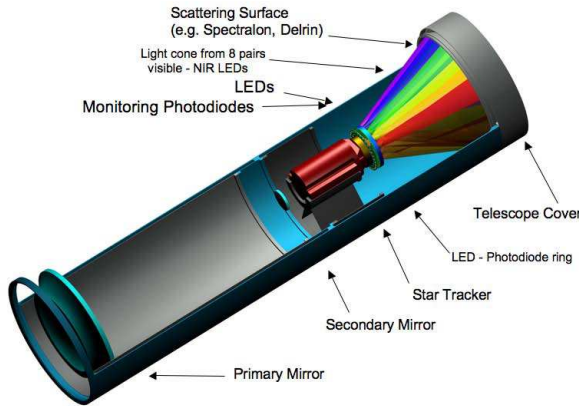


Figure 11. The OCM LEDs are mounted in an annular ring about the star tracker behind the secondary mirror and they illuminate a diffuser on the inside of the telescope cover which in turn illuminates the telescope primary with an angular distribution of rays.

Sources (SIRCUS) facility.^{44,16} The second method determines the sensitivity from the illumination of the telescope with a continuum source configured to have the same power and spectral distribution as the stellar source.

6. CALIBRATION MONITORING

The key to a successful calibration experiment is knowledge of the absolute sensitivity of the instrument at the moment the targets are observed. Although an end-to-end absolute recalibration of the instrument will be performed after each launch, there is a post-launch and pre-launch time lag before this calibration can be performed. Consequently, an On-board Calibration Monitor (OCM) calibration has been developed to track the payload for any changes in sensitivity from the moment that the payload is calibrated, through ground processing and launch, and in-flight, immediately after the observation is completed and prior to touch-down.

On-board Calibration Monitor – OCM The current baseline design (Fig. 11) of the OCM uses 8 pairs of feedback stabilized LEDs, with central wavelengths spanning the ACCESS bandpass, to illuminate the telescope by scattering off a diffuser mounted on the interior of the telescope cover.⁴⁵ The LEDs are located in a multi-layer annular assembly mounted as a collar around the nose of the

star tracker positioned behind the secondary mirror of the telescope. This assembly does not increase the central obscuration of the cassegrain telescope. LEDs were selected as the light source for the OCM because they are compact, low-mass, and consume little power. Feedback stabilization is achieved through brightness monitoring of each LED by an adjacent dedicated photodiode, which views its LED through its transparent sidewall. Laboratory data has been acquired for a subset of the flight candidate LEDs as a function of wavelength and temperature (e.g. Figs. 12 & 13). The OCM will monitor instrument performance during the end-to-end transfer of the NIST calibration of the diode standards to ACCESS in the laboratory. This will provide the necessary transfer in sensitivity to the spectrograph detector to compare against subsequent monitoring observations of the OCM during the various I&T phases. This light source will provide the capability to switch on-off during an observation to check the detector dependence on count rate. The use of the OCM will provide real time and up-to-date knowledge of the ACCESS sensitivity.

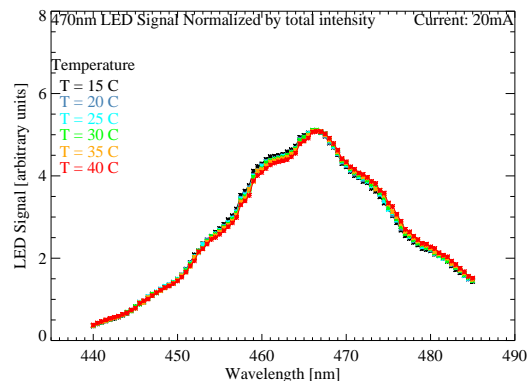


Figure 12. The spectral energy output of the LED as a function of temperature is shown for the 470nm LED. The total intensities have been normalized to common values, representing the effect of feedback control.⁴⁵

6.1 Error Budget

ACCESS will establish the absolute spectrophotometric calibration of a set of stars to better than 1% precision across a $0.35 < \lambda < 1.7 \mu\text{m}$ bandpass with a resolving power of 500. A fraction of the error budget will be allocated to the statistical uncertainty associated with the observation of the standard star itself; the remainder of the error budget will be comprised of the systematic uncertainties in the instrument calibration. Each of the primary targets will be observed twice with a S/N of 200 per resolution

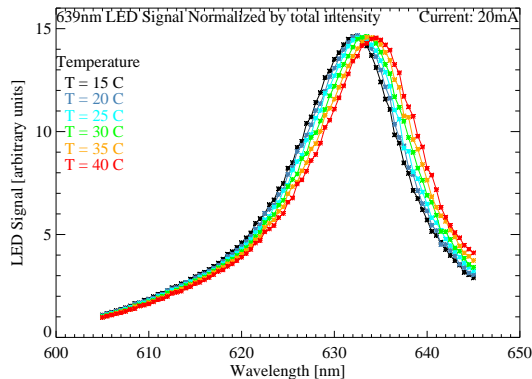


Figure 13. The spectral energy output of the LED as a function of temperature is shown for the 639nm LED. The total intensities have been normalized to common values, representing the effect of feedback control.⁴⁵

element for at least one of the two measurements. This yields a statistical uncertainty in the flux measurement of 0.5% for each resolution element. If we attribute the statistical uncertainty in our error budget to the counting statistics per resolution element, then the error budget available for the quadrature sum of our systematic uncertainties is 0.86%.

However, it is the slope of the flux distribution as a function of wavelength (aka “the color”) that must be precisely determined over the bandpass of interest. The number of spectral elements contributing to the “bandpass of interest” is intermediate between our single resolution element ($\Delta\lambda$) and the full spectral range of the instrument. Each of these spectral elements effectively contributes a measurement of the slope. This ensemble of measurements sampling the slope at each wavelength resolution element in the bandpass reduces the uncertainty in the overall measurement.

Conservatively, the sum of our systematic uncertainties must be less than 0.86%. Some margin is provided by the requirement that it is the slope, not an individual resolution element, that must be known precisely. This fraction of the error budget will be devoted to the precise calibration of our instrument and the transfer of this calibration from NIST calibrated photodiode detectors.

Calibration measurements will be performed repeatedly, with and without variations in the procedure, to identify and quantify sources of systematic error and to establish repeatability and quantify errors. Standard stars are planned to be observed at least twice each.

Using error estimates from the literature, performance specifications, measurements, or experi-

ence with other ground and space based instruments, we have identified and tabulated expected sources of uncertainty. Quantifying their contribution to our error budget, we estimate a total uncertainty of 0.59%(visible) to 0.73%(NIR) for our identified systematic errors. Based upon a worst-case systematic error budget of 0.86%, a total identified uncertainty of 0.73% leaves a margin of 0.47% for unidentified sources of uncertainty or as margin for the calibration of the dark energy mission itself.

From this, it is apparent that *although an absolute measurement to 1% precision is challenging, with rigorous attention to detail this goal can be met.*

7. SUMMARY

ACCESS is a sub-orbital program that will enable a fundamental calibration of the spectral energy distribution of bright primary standard stars, as well as stars 10 magnitudes fainter, in physical units through a direct comparison with NIST traceable irradiance (detector) standards. Each star will be observed on two separate rocket flights to verify repeatability to < 1%, an essential element in establishing standards with 1% precision.

Using irradiance standards to place these stellar observations on an absolute scale in physical units is our primary goal. However, despite possible errors caused by using model calculations for fundamental absolute flux standards, modeling the target stars is also an essential component of our proposed program.

Any unexplained deviation of our NIST traceable fluxes from the models would be a strong indicator of some error in our results. Models can be fit to agree with the observations over the measured 0.35-1.7 μm range and then used to predict the flux beyond these wavelength limits. Producing a model with a good fit over a long baseline of medium resolution spectroscopy greatly improves confidence in the predicted fluxes, especially in comparison with models that are fit to just a few broadband photometry points. Thus, ACCESS will establish to 1% precision a direct absolute calibration of standard stars across the 0.35 – 1.7 μm bandpass and enable the validation of high resolution models of fundamental standards for use by space and ground observatories.

ACKNOWLEDGMENTS

We would like to thank K. Lykke, T. Larason, S. Brown, and G. Fraser for helpful discussions re-

garding the NIST calibration facilities. This research is being funded through NASA APRA-2007 and DOE DE-PS02-07ER07-08, with the ACCESS program support provided through NASA APRA-2007.

REFERENCES

- [1] Riess, A. et al. *A. J.* **117**, 707 (1999).
- [2] Perlmutter, S. et al., “Measurements of Omega and Lambda from 42 High-Redshift Supernovae,” *Ap. J.* **517**, 565–586 (June 1999).
- [3] Perryman, M. A. C., de Boer, K. S., Gilmore, G., Høg, E., Lattanzi, M. G., Lindegren, L., Luri, X., Mignard, F., Pace, O., and de Zeeuw, P. T., “GAIA: Composition, formation and evolution of the Galaxy,” *A&A* **369**, 339–363 (Apr. 2001).
- [4] Kaiser, M. E., Kruk, J. W., McCandliss, S. R., Sahnou, D. J., Rauscher, B. J., Benford, D. J., Bohlin, R. C., Deustua, S. E., Dixon, W. V., Feldman, P. D., Gardner, J. P., Kimble, R. A., Kurucz, R., Lampton, M., Moos, H. W., Perlmutter, S., Riess, A. G., Woodgate, B. E., and Wright, E. L., “ACCESS: absolute color calibration experiment for standard stars,” *SPIE Conference Series* **7014** (Aug. 2008).
- [5] Kent, S., Kaiser, M. E., Deustua, S. E., Smith, J. A., et al., “Photometric Calibrations for 21st Century Science,” *Astronomy* **2010**, 8 (2009).
- [6] Riess, A. et al. *ApJ. Lett.* **600**, L163 (2004).
- [7] Riess, A. G. et al., “Type Ia Supernova Discoveries at $z > 1$ from the Hubble Space Telescope: Evidence for Past Deceleration and Constraints on Dark Energy Evolution,” *Ap. J.* **607**, 665–687 (June 2004).
- [8] Knop, R. A. et al. *Ap. J.* **598**, 102 (2003).
- [9] Tonry, J. L. et al. *Ap. J.* **594**, 1 (2003).
- [10] Hamuy, M., Phillips, M. M., Suntzeff, N. B., Schommer, R. A., Maza, J., and Aviles, R. *A. J.* **112**, 2391 (1996).
- [11] Linder, E. V. and Huterer, D. *Physical Review D* **67**, 1303L (2003).
- [12] Astier, P., “Supernova cosmology and dark energy,” in [*SPIE Astronomical Instrumentation*], SPIE, ed., SPIE, Bellingham, Washington (2008).
- [13] Yoon, H. W., Proctor, J. E., and Gibson, C. E., “FASCAL 2: a new NIST Facility for the Calibration of the Spectral Irradiance of Sources,” *Metrologia* **40**, 30 (Feb. 2003).
- [14] Yoon, H. W., Butler, J. J., Larason, T. C., and Eppeldauer, G. P., “Linearity of InGaAs Photodiodes,” *Metrologia* **40**, 154 (Feb. 2003).
- [15] Yoon, H. W., Dopkiss, M. C., and Eppeldauer, G. P., “Performance Comparisons of InGaAs, Extended InGaAs, and Short-wave HgCdTe Detectors between 1 μm and 2.5 μm ,” *SPIE Conference Series* **6297** (Sept. 2006).
- [16] Brown, S. W., Eppeldauer, G. P., and Lykke, K. R., “Facility for spectral irradiance and radiance responsivity calibrations using uniform sources,” *Appl. Opt.* **45**, 8218–8237 (Nov. 2006).
- [17] Brown, S. W., Smith, A. W., Woodward, J. T., and Lykke, K. R., “Characterization, Calibration, and Performance Validation of Imaging Sensors at NIST: the SIRCUS Facility,” in [*18th Annual CALCON Technical Conference*], CALCON, ed., Utah State Research Foundation, Logan, UT (2009).
- [18] Bohlin, R. C., “Hst stellar standards with 1% accuracy in absolute flux,” in [*The Future of Photometric, Spectrophotometric and Polarimetric Standardization*], Sterken, C., ed., 315, APS Conference Series, Baltimore (2007).
- [19] Thuillier, G., Herse, M., Labs, D., Foujols, T., Peetermans, W., Gillotay, D., Simon, P. C., and Mandel, H. *Solar Physics* **214**, 1–22 (2003).
- [20] Bohlin, R. C. and Gilliland, R. L., “Hubble Space Telescope Absolute Spectrophotometry of Vega from the Far-Ultraviolet to the Infrared,” *A. J.* **127**, 3508 (jun 2004).
- [21] Cohen, M., Walker, R. G., Barlow, M. J., and Deacon, J. R., “Spectral irradiance calibration in the infrared. I - Ground-based and IRAS broadband calibrations,” *A. J.* **104**, 1650–1657 (Oct. 1992).
- [22] Cohen, M., Wheaton, W. A., and Megeath, S. T., “Spectral Irradiance Calibration in the Infrared XIV The Absolute Calibration of 2MASS,” *A. J.* **126**, 1090–1096 (Aug. 2003).
- [23] Cohen, M., “Nir stellar standards,” in [*The Future of Photometric, Spectrophotometric and Polarimetric Standardization*], Sterken, C., ed., 999, APS Conference Series, Baltimore (2007).
- [24] Rieke, G. et al., “Absolute Physical Calibration in the Infrared,” *A. J.* **135**, 2245–2263 (June 2008).
- [25] Hayes, D. S., “Stellar absolute fluxes and energy distributions from 0.32 to 4.0 microns,” in [*IAU Symp. 111: Calibration of Fundamental*

- Stellar Quantities*], 225–249, Reidel, Dordrecht (1985).
- [26] Fraser, G. T., Brown, S. W., Yoon, H. W., Johnson, B. C., and Lykke, K. R., “Absolute flux calibrations of stars,” *SPIE Conference Series* **6678** (Oct. 2007).
- [27] Woodward, J. T., Smith, A. W., Lykke, K. R., Jenkins, C., and Lin, C., “High-accuracy Telescope Calibration Facility at NIST,” in [*18th Annual CALCON Technical Conference*], CALCON, ed., Utah State Research Foundation, Logan, UT (2009).
- [28] Zimmer, P. C., McGraw, J. T., and MAP Research Group, “Measurement Astrophysics (MAP) First Steps: Precision Measurements of Atmospheric Extinction,” in [*18th Annual CALCON Technical Conference*], CALCON, ed., Utah State Research Foundation, Logan, UT (2009).
- [29] Stubbs, C. W., High, F. W., George, M. R., DeRose, K. L., Blondin, S., Tonry, J. L., Chambers, K. C., Granett, B. R., Burke, D. L., and Smith, R. C., “Toward More Precise Survey Photometry for PanSTARRS and LSST: Measuring Directly the Optical Transmission Spectrum of the Atmosphere,” *Pub. Astron. Soc. Pacific* **119**, 1163–1178 (Oct. 2007).
- [30] McGraw, J. T., Stubbs, C. W., Zimmer, P. C., Fraser, G. T., and Vivekanandan, J., “Measurement Astrophysics (MAP) First Steps: A New Decade of Ground-based Photometric Precision and Accuracy,” *Astronomy* **2010**, 34 (2009).
- [31] Burke, D. and LSST Collaboration, “Calibration of LSST Instrument and Data,” *Bulletin of the American Astronomical Society* **41**, 369 (Jan. 2009).
- [32] Blackwell, D. E., Leggett, S. K., Petford, A. D., Mountain, C. M., and Selby, M. J., “Absolute calibration of the infrared flux from VEGA at 1.24, 2.20, 3.76 and 4.6 microns by comparison with a standard furnace,” *MNRAS* **205**, 897–905 (Dec. 1983).
- [33] Selby, M. J., Mountain, C. M., Blackwell, D. E., Petford, A. D., and Leggett, S. K., “Measurement of the absolute monochromatic flux from VEGA at 2.20 and 3.80 microns by comparison with a furnace,” *MNRAS* **203**, 795–800 (May 1983).
- [34] Mountain, C. M., Selby, M. J., Leggett, S. K., Blackwell, D. E., and Petford, A. D., “Measurement of the absolute flux from VEGA at 4.92 microns,” *AAP* **151**, 399–402 (Oct. 1985).
- [35] Stubbs, C. W. and Tonry, J. L., “Toward 1% Photometry: End-to-End Calibration of Astronomical Telescopes and Detectors,” *Ap. J.* **646**, 1436–1444 (Aug. 2006).
- [36] Oke, J. B. and Schild, R. E., “The Absolute Spectral Energy Distribution of Alpha Lyrae,” *Ap. J.* **161**, 1015 (Sept. 1970).
- [37] Hayes, D. S. and Latham, D. W., “A rediscussion of the atmospheric extinction and the absolute spectral-energy distribution of VEGA,” *Ap. J.* **197**, 593–601 (May 1975).
- [38] Larason, T. C. and Houston, J. M., “Spectroradiometric Detector Measurements Ultraviolet, Visible, and Near-infrared Detectors for Spectral Power,” (2008).
- [39] Moreels, G., Megie, G., Vallance Jones, A., and Gattinger, R. L., “An oxygen-hydrogen atmospheric model and its application for the OH emission problem,” *Journal of Atmospheric and Terrestrial Physics* **39**, 551–570 (1977).
- [40] Reach, W. T., Megeath, S. T., Cohen, M., Hora, J., Carey, S., Surace, J., Willner, S. P., Barmby, P., Wilson, G., Glaccum, W., Lowrance, P., Marengo, M., and Fazio, G. G., “Absolute Calibration of the Infrared Array Camera on the Spitzer Space Telescope,” *PASP* **117**, 978–990 (Sept. 2005).
- [41] Bohlin, R. C. and Gilliland, R. L., “Absolute Flux Distribution of the SDSS Standard BD17D4708,” *A. J.* **128**, 3053–3060 (dec 2004).
- [42] McCandliss, S. R., Martinez, M. E., Feldman, P. D., Pelton, R., Keski-Kuha, R. A., and Gum, J. S., “Design and fabrication of a 40-cm-diameter SiC-coated normal incidence telescope and spectrometer,” in [*Proc. SPIE Vol. 2011, Multilayer and Grazing Incidence X-Ray/EUV Optics II*], 310–321 (1994).
- [43] Shaw, P.-S., Larason, T. C., Gupta, R., Brown, S. W., and Lykke, K. R., “Improved Near-Infrared Spectral Responsivity Scale,” (2000).
- [44] Brown, S. W., Eppeldauer, G. P., Rice, J. P., Zhang, J., and Lykke, K. R., “Spectral Irradiance and Radiance responsivity Calibrations using Uniform Sources (SIRCUS) facility at NIST,” in [*Earth Observing Systems IX*], Barnes, W. L. and Butler, J. J., eds., *SPIE* **5542**, 363–374 (Oct. 2004).
- [45] Kruk, J. W., Kaiser, M. E., McCandliss, S. R., et al., “On-board Calibration Monitor for Tracking Instrument Sensitivity,” in [*SPIE Astronomical Instrumentation*], 7014, S., ed., 115, SPIE, Bellingham, Washington (2008).